

## JES FOCUS ISSUE ON PROTON EXCHANGE MEMBRANE FUEL CELL (PEMFC) DURABILITY

# Highly Durable, Cost-Effective, and Multifunctional Carbon-Supported IrRu-Based Catalyst for Automotive Polymer Electrolyte Fuel Cell Anodes

Eunyoung You, 1,a Myoungki Min, 1 Seon-Ah Jin, 2,b Taeyoon Kim, 1,c and Chanho Pak 63,\*,z

The design of highly durable, electroactive, and cost-effective catalysts to replace the currently prevalent Pt-based ones has long been a major milestone for expanding the market penetration of fuel cell electric vehicles (FCEVs). Over the past decades, catalyst degradation in automotive fuel cells under transient conditions (e.g., startup/shutdown and cell reversal) has attracted much attention due to its irreversible consequences for the membrane electrode assembly (MEA). Herein, we evaluate  $IrRu_n/C$  as alternative catalysts to increase MEA anode durability under cell reversal conditions and investigate their suitability for use in FCEVs. Among the various Ir:Ru ratios, the best hydrogen oxidation activity was observed for Ir:Ru = 1:4 (mol/mol), as confirmed by rotating disk electrode measurements. The performances of  $IrRu_4/C$  and Pt/C as anode catalysts were compared side by side, with the corresponding I-V and anode polarization tests carried out under various operating conditions (cell temperature, relative humidity, and backpressure). Importantly,  $IrRu_4/C$  showed Pt-comparable ( $\sim 100\%$ ) MEA performance and hydrogen oxidation activity, additionally exhibiting a  $\sim 120$  times better durability under cell reversal conditions.

© The Author(s) 2018. Published by ECS. This is an open access article distributed under the terms of the Creative Commons Attribution 4.0 License (CC BY, http://creativecommons.org/licenses/by/4.0/), which permits unrestricted reuse of the work in any medium, provided the original work is properly cited. [DOI: 10.1149/2.0121806jes]

Manuscript submitted December 22, 2017; revised manuscript received February 22, 2018. Published March 5, 2018. This paper is part of the JES Focus Issue on Proton Exchange Membrane Fuel Cell (PEMFC) Durability.

Polymer electrolyte membrane fuel cells (PEMFCs) are a promising power source for next-generation eco-friendly vehicles due to featuring high energy density, high conversion efficiency, and zero  $\mathrm{CO}_2$  emission, thus being superior to conventional energy sources. Nevertheless, the high cost and durability issues of PEMFC catalysts still hamper the commercialization of fuel cell electric vehicles (FCEVs).

Recently, much effort has been directed at finding affordable alternatives to Pt-based catalysts exclusively used in both the anode and the cathode of the membrane electrode assembly (MEA). However, the above attempts have rarely been successful in achieving Pt-comparable MEA performances, with the replacement of Pt-based catalysts by non-Pt ones being more tangible for the hydrogen oxidation reaction (HOR) at the anode, as demonstrated by numerous studies. <sup>1–5</sup> Moreover, carbon-supported Ir-based bimetallic catalysts, IrV/C² and IrCo/C, <sup>4</sup> have been successfully applied as anode catalysts for PEMFCs.

The exploitation of durable catalysts is crucial for the prevention of fuel cell performance degradation during transient conditions such as startup/shutdown (SU/SD) and cell reversal (CR), being a topic extensively discussed in the fuel cell community in view of its potential automobile applications.  $^{6,7}$  During the lifetime of an FCEV ( $\sim\!5,000$  operation hours), the SU/SD and the CR occur approximately 5,000 and 200 times, respectively.  $^6$ 

During the SU/SD of an FCEV, gas flushing results in air/fuel boundary formation, allowing the oxygen reduction reaction (ORR) to take place at the anode side of the MEA still exposed to air, with the required protons being supplied by the cathode. As a result, the carbon support of the cathode is oxidized, and the cathode experiences positive potentials of up to 1.8 V vs. the normal hydrogen electrode (NHE).<sup>7,8</sup> Therefore, repeated SU/SD conditions induce both seri-

ous carbon corrosion and cathode catalyst degradation. Several approaches to mitigating carbon corrosion at the cathode have been suggested, e.g. the use of highly graphitized carbon and/or metal oxides as supporting materials, 8-11 alteration of stack operations for preventing air/fuel boundary formation, 12 and the utilization of oxygen evolution reaction (OER) catalysts as additives for protecting the cathode catalyst from carbon corrosion. 13-17 Ultimately, using an ORR-inactive, yet HOR-active anode catalyst is expected to fundamentally prevent this detrimental phenomenon.

Fuel starvation during fuel cell operation can be caused by numerous factors, e.g., water flooding within the fuel cell, ice formation in winter, abnormal operation of the reactant gas supplier, etc. 18 Once fuel starvation breaks out, one or more cells in the stack can experience cell reversal conditions, under which the carbon support of the anode is oxidized, with repetitive CR resulting in the irreversible degradation of MEA performance. Since the Pt loading of the anode is much lower than that of the cathode, the anode catalyst layer is usually thinner than its cathode counterpart, implying that carbon corrosion is more damaging to the anode. Other than a systematic solution, approaches similar to those adopted for SU/SD mitigation, i.e., the use of highly graphitized carbon and/or metal oxides as supporting materials, have been applied to mitigate instability under CR conditions.<sup>7</sup> The use of anode catalyst layer additives such as Ir, Ru, or their oxide forms was also shown to decrease the above performance deterioration.<sup>7,15</sup> Upon the occurrence of CR, these additives facilitate the OER (Equation 1) instead of promoting the carbon oxidation reaction (COR, Equation 2), inhibiting the collapse of the anode carbon support. 17,18

$$2H_2O \rightarrow O_2 + 4H^+ + 4e^ E^{\circ} = 1.23 \text{ V vs. RHE}$$
 [1]

$$C + 2H_2O \rightarrow CO_2 + 4H^+ + 4e^ E^\circ = 0.21 \text{ V vs. RHE}$$
 [2]

Herein, we perform an in-depth characterization of IrRu<sub>4</sub> supported on carbon (hereafter denoted as IrRu<sub>4</sub>/C), using it as an HOR- and OER-active and moderately ORR-active catalyst to meet the cost and durability demands of MEAs intended for use in FCEVs. Although the commercial unavailability of IrRu<sub>4</sub>/C does not allow a direct cost

<sup>&</sup>lt;sup>1</sup>Fuel Cell Group, Battery R&D Center, Samsung SDI, Yeongtong-gu, Suwon, Gyeonggi-do 16678, Korea

<sup>&</sup>lt;sup>2</sup>Energy Lab, Samsung Advanced Institute of Technology, Samsung Electronics Co., Ltd., Yeongtong-gu, Suwon, Gyeonggi-do 16678, Korea

<sup>&</sup>lt;sup>3</sup> Graduate Program of Energy Technology, School of Integrated Technology, Institute of Integrated Technology, Gwangju Institute of Science and Technology, Gwangju 61005, Korea

<sup>\*</sup>Electrochemical Society Member.

<sup>&</sup>lt;sup>a</sup>Present address: Core Eco-Technology Team, R&D Division, Hyundai Mobis, Co. Ltd., Giheung-gu, Yongin, Gyeonggi-do 16891, Korea.

<sup>&</sup>lt;sup>b</sup>Present address: School of Materials Engineering, Purdue University, West Lafayette, Indiana 47907, USA.

<sup>&</sup>lt;sup>c</sup>Present address: Dongjin Semichem, Seo-gu, Incheon 22824, Korea.

<sup>&</sup>lt;sup>z</sup>E-mail: chanho.pak@gist.ac.kr

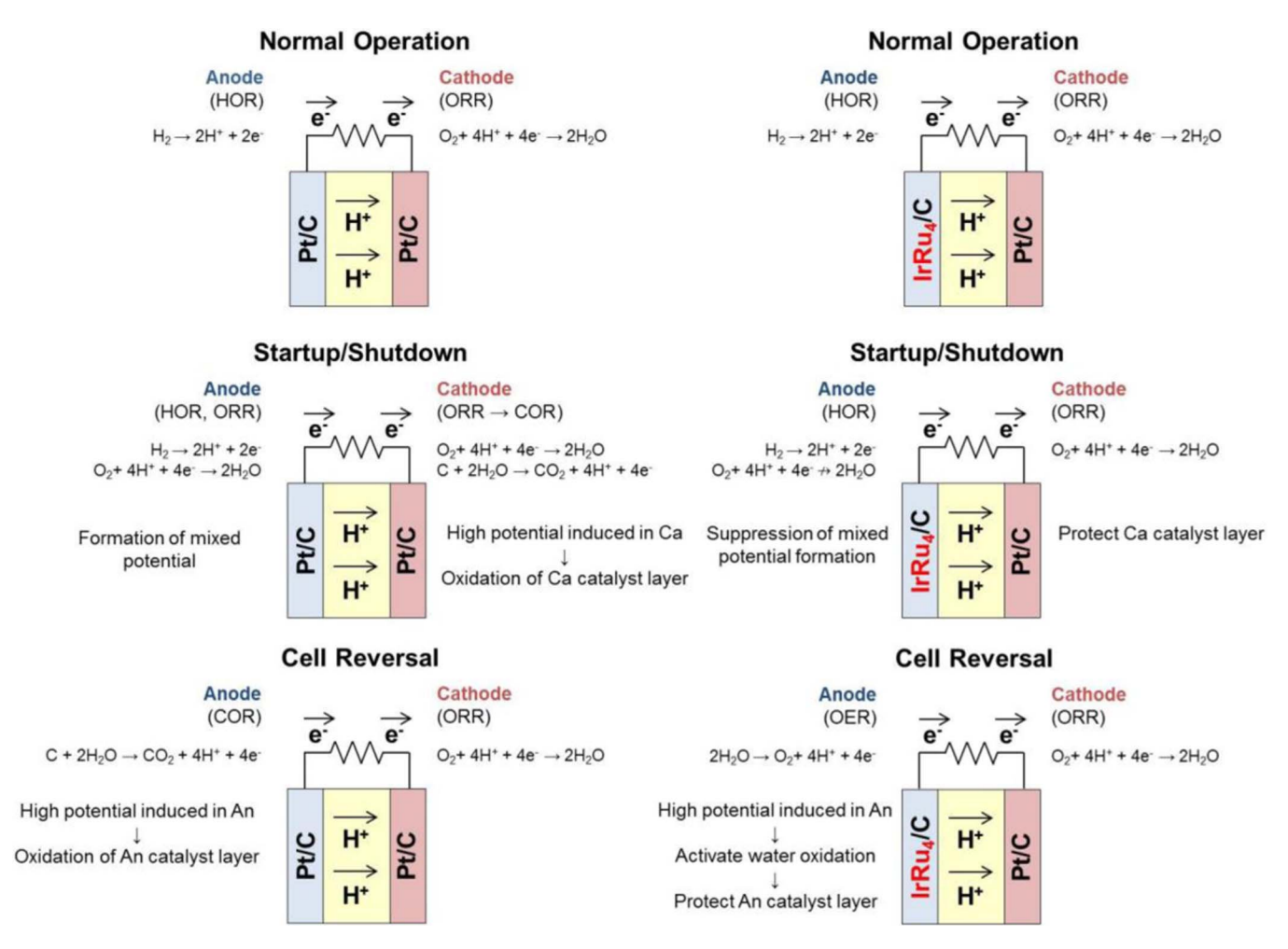


**Figure 1.** Prospective benefits of replacing a Pt/C anode with an IrRu<sub>4</sub>/C anode in PEMFCs used for powering FCEVs: 1) cost reduction (65% that of Pt) with unchanged performance, 2) cathode layer protection during startup/shutdown, 3) anode layer protection during cell reversal. An and Ca stand for anode and cathode, respectively.

comparison with carbon-supported Pt (Pt/C), the base metal price per unit mass of the former equals approximately 22% that of Pt/C (262.41 vs. 1185.01 \$/oz),  $^{19}$  showing the cost competitiveness of IrRu<sub>4</sub> over Pt. Additionally we discuss the *I-V* performance and CR tolerance of IrRu<sub>4</sub>/C and commercial Pt/C anode MEAs, with the ultimate objective of this work illustrated in Fig. 1.

### **Experimental**

Preparation of IrRu<sub>4</sub> catalysts.—Two different types of carbon supports were used: commercially available Ketjen black (KB) carbon 300J and KB thermally treated in-house above 2250°C (GKB). IrRu<sub>4</sub> catalysts loaded on carbon supports were prepared by simple impregnation followed by reduction in an atmosphere of H<sub>2</sub>/N<sub>2</sub> in a tube furnace at 573 K to obtain a 30 wt% precious group metal (PGM) loading with a nominal ratio of Ir:Ru = 1:4 (mol/mol). Dihydrogen hexachloroiridate (IV) hydrate and ruthenium (III) chloride hydrate (both purchased from Heraeus) were used as Ir and Ru precursors, respectively. Impregnation was performed by dispersing the carbon support powder in ethanol under ultrasonication followed by vortexadmixing of ethanolic solutions of Ir and Ru precursors. After vigorous mixing, the solution was concentrated in vacuo, and the residue was dried at 353 K overnight. The obtained solids were mortar-pestled and finally reduced at 573 K in a tube furnace in a flow of H<sub>2</sub>/N<sub>2</sub>. The obtained catalysts were denoted as IrRu<sub>4</sub>/KB and IrRu<sub>4</sub>/GKB according to the type of the carbon support.

*Physicochemical characterization.*—As-synthesized IrRu<sub>4</sub>/C catalysts were characterized by X-ray diffraction (XRD), transmission electron microscopy (TEM), thermogravimetric analysis (TGA), and inductively coupled plasma-atomic emission spectrometry (ICP-AES). Powder XRD patterns were collected using a Philips X'Pert Pro X-ray diffractometer equipped with a Cu  $K_α$  radiation source. The mean crystallite size was calculated based on the full width at half maximum of the deconvoluted main peak utilizing the Scherrer equation. An FE-TEM TECNAI microscope (F30, FEI) operated at an accelerating voltage of 300 kV was used to confirm particle size and distribution. ICP-AES was used to determine the contents of Ir, Ru, and carbon, and TGA (Rubotherm) was used to estimate the metal loading of the catalyst.

Rotating disk electrode half-cell test.—Commercial Pt/C and assynthesized carbon-supported IrRu<sub>4</sub> anode catalysts were electrochemically analyzed in half-cell configuration using a rotating disk electrode (RDE) apparatus (potentiostat/galvanostat model 2273A, Princeton Applied Research) in 0.1 M aqueous HClO<sub>4</sub> at 298 K. In all half-cell tests, Pt mesh was used as a counter electrode, and Ag/AgCl (0.197 V vs. NHE) was used as a reference electrode. A commercial Pt/C catalyst (47.2 wt% Pt) was chosen as a reference. Depending on the purpose of the electrochemical test, the preparation of the catalyst ink for the working electrode and the test procedure were slightly varied.

For HOR activity measurement, the catalyst ink was prepared by ultrasonically dispersing 20 mg of each catalyst (Pt/C and IrRu<sub>4</sub>/KB)

in 10 mL of deionized water. Subsequently, 15  $\mu$ L of the catalyst ink was dropped onto a polished glassy carbon disk (geometric surface area = 0.196 cm²), and 15  $\mu$ L of 0.05 wt% aqueous Nafion solution (Aldrich) was dropped on top to fix the catalyst layer. Catalyst activation prior to activity measurement was achieved by performing cyclic voltammetry (CV) tests in a potential range of -0.01-0.6 V vs. Ag/AgCl at a scan rate of 100 mV/s for 20 cycles in N<sub>2</sub>-saturated 0.1 M aqueous HClO<sub>4</sub>. HOR activity was determined by chronoamperometry at a fixed potential of 20 mV and various rotation speeds (400, 900, 1600, and 2500 rpm) in H<sub>2</sub>-saturated 0.1 M aqueous HClO<sub>4</sub>. During chronoamperometric tests, the limiting oxidation current was stabilized and measurements were conducted for 180 s. The kinetic currents  $i_k$  at 20 mV (vs. NHE) were calculated from Koutecky-Levich plots.<sup>20</sup>

For ORR and OER activity measurements, an appropriate amount of the catalyst ink (prepared in a similar way) was dropped onto the glassy carbon electrode to achieve a loading of  $17 \,\mu g_{PGM}/cm^2$ . After the PGM layer was dried,  $7 \,\mu L$  of  $0.05 \,\text{m}\,\text{m}$  Nafion solution was dropped on top as a cover layer. For catalyst activation, CV tests were performed in a potential range of  $-0.23-0.6 \,\text{V}$  vs. Ag/AgCl at a scan rate of  $200 \,\text{m}\,\text{V/s}$  for  $100 \,\text{cycles}$  in  $N_2$ -saturated  $0.1 \,\text{M}$  HClO $_4$ . ORR activities were determined in  $O_2$ -saturated solution, and CV and linear sweep voltammetry (LSV) tests were performed at a rotation speed of  $1600 \,\text{rpm}$  while the solution was purged with a copious amount of  $O_2$ . OER activity measurements were performed in  $N_2$ -purged electrolyte solution, with the rest of the testing procedure being identical to that used for ORR. The LSV measurement was performed in a potential range of  $0.7-1.5 \,\text{V}$  vs. Ag/AgCl at a rate of  $5 \,\text{m}\,\text{V/s}$ .

MEA preparation.—Commercial 20 wt% Pt/C (TEC10EA20E, TKK) and 52 wt% PtCo/C (TEC36F52, TKK) were chosen as reference Pt anode and cathode catalysts, respectively, and as-synthesized 30 wt% IrRu<sub>4</sub>/GKB was applied as an anode catalyst. The catalyst slurry was prepared by ballmilling a mixture of catalyst powder, appropriate amount of perfluorosulfonic acid-type ionomer dispersion, organic solvent, and deionized water; the solid content of the slurry (10–13 wt%) was sufficient to prevent particle sedimentation. The prepared slurry was coated onto decal films and dried in an oven at 60°C overnight. A catalyst-coated membrane with an active area of 26 cm<sup>2</sup> was fabricated by placing a 12-μm-thick perfluorosulfonic acid-polytetrafluoroethylene based membrane between the anode and cathode catalyst layers using the decal transfer technique. The cathode and anode Pt loadings equaled 0.18 and 0.02 mg/cm<sup>2</sup>, respectively, while a PGM loading of 0.06 mg/cm<sup>2</sup> was used for the IrRu<sub>4</sub>/C anode. Finally, MEA fabrication was completed by attaching gas diffusion layers on both sides of the electrodes.

MEA evaluation: I-V performance and anode polarization.—After installing the MEA in the fuel cell housing, its performance was analyzed using an electrochemical test station (Scitech Korea Co. Inc.) at (i) 65°C, 100% relative humidity (RH), ambient pressure, and (ii) 90°C, 50% RH, 150 kPa backpressure. Hydrogen and air fuel gases were supplied at stoichiometric ratios (SRs) of 1.5 and 2.0, respectively, for ambient pressure testing, with the corresponding values for back-pressurized conditions equaling 1.2 and 2.0. To compare the HOR activities of the two anode catalysts, anode polarization curves were recorded for both MEAs at currents of up to 20 A under the abovementioned conditions in a flow of H<sub>2</sub> (228 sccm) at both electrodes.

Anode durability test: cell reversal.—The anode durability of MEAs was tested by intentionally inducing fuel starvation at the anode to induce CR. To simulate fuel starvation,  $N_2$  was flown in the anode side in place of  $H_2$ . Single-cell MEAs were operated at 65°C, 50% RH, and ambient pressure with anode and cathode SRs equaling 1.2 and 2.0, respectively. The current density was set to 0.2 A/cm², and the time required to reach  $-2.0 \text{ V}(t_{CR})$  was used as an index of CR tolerance.

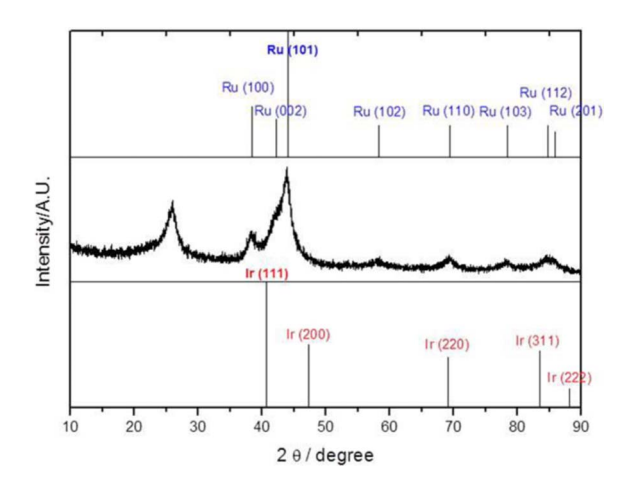


Figure 2. XRD pattern of as-synthesized IrRu<sub>4</sub>/GKB and its comparison with those of Ir (JCPDS Card No. 06-0598) and Ru (06-0663).

#### **Results and Discussion**

Physicochemical characterization of IrRu<sub>4</sub>/C.—Figure 2 shows the XRD pattern of as-synthesized IrRu<sub>4</sub>/GKB, with the recorded peaks deconvoluted using ProFit software (Philips Electronics). Comparison of the above pattern with those of Ir (JCPDS Card No. 06-0598) and Ru (06-0663) showed that the main peak at  $2\theta = 43.903^{\circ}$ was slightly shifted compared to that of Ru (101) ( $2\theta = 44.007^{\circ}$ ). Moreover, the peak around 69.233° lied between those of Ir (220) (2 $\theta$ = 69.144°) and Ru (110) ( $2\theta = 69.407$ °). Thus, the obtained results strongly suggested the occurrence of Ir and Ru alloying. Due to its high Ru content, IrRu4 adopted the hexagonal close-packed crystal structure of Ru, with Scherrer analysis of the XRD peak at  $\sim$ 69° affording an average crystallite size of ~4.7 nm. TEM imaging (Fig. 3) showed that metal nanoparticles were well dispersed on the graphitic carbon support, and ICP analysis confirmed that the synthesized IrRu<sub>4</sub>/GKB catalyst contained Ir and Ru in a ratio close to 1:4 (mol/mol). TGA (performed in air at temperatures of up to 800°C) revealed that the PGM loading of the above catalyst equaled 28.8 wt%, being close to the target loading of 30 wt%.

Comparison of Pt/C and IrRu<sub>4</sub>/C catalysts using RDE tests.— HOR activity testing.—A separate RDE half-cell study of HOR activity performed by Jin et al.<sup>21</sup> showed that among the various Ir:Ru

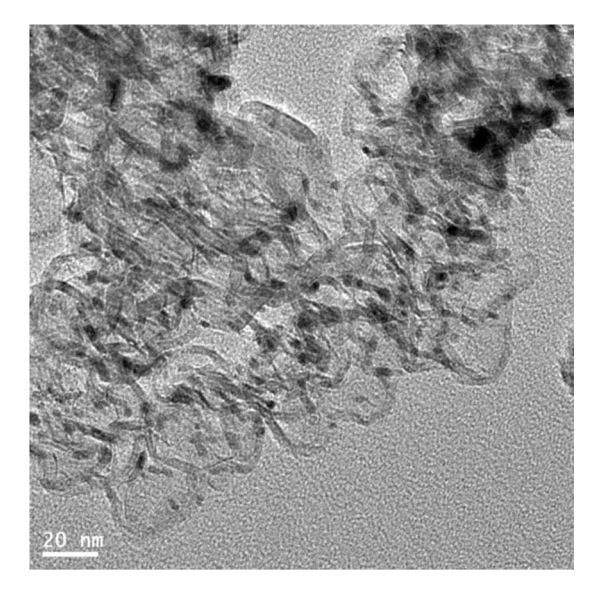
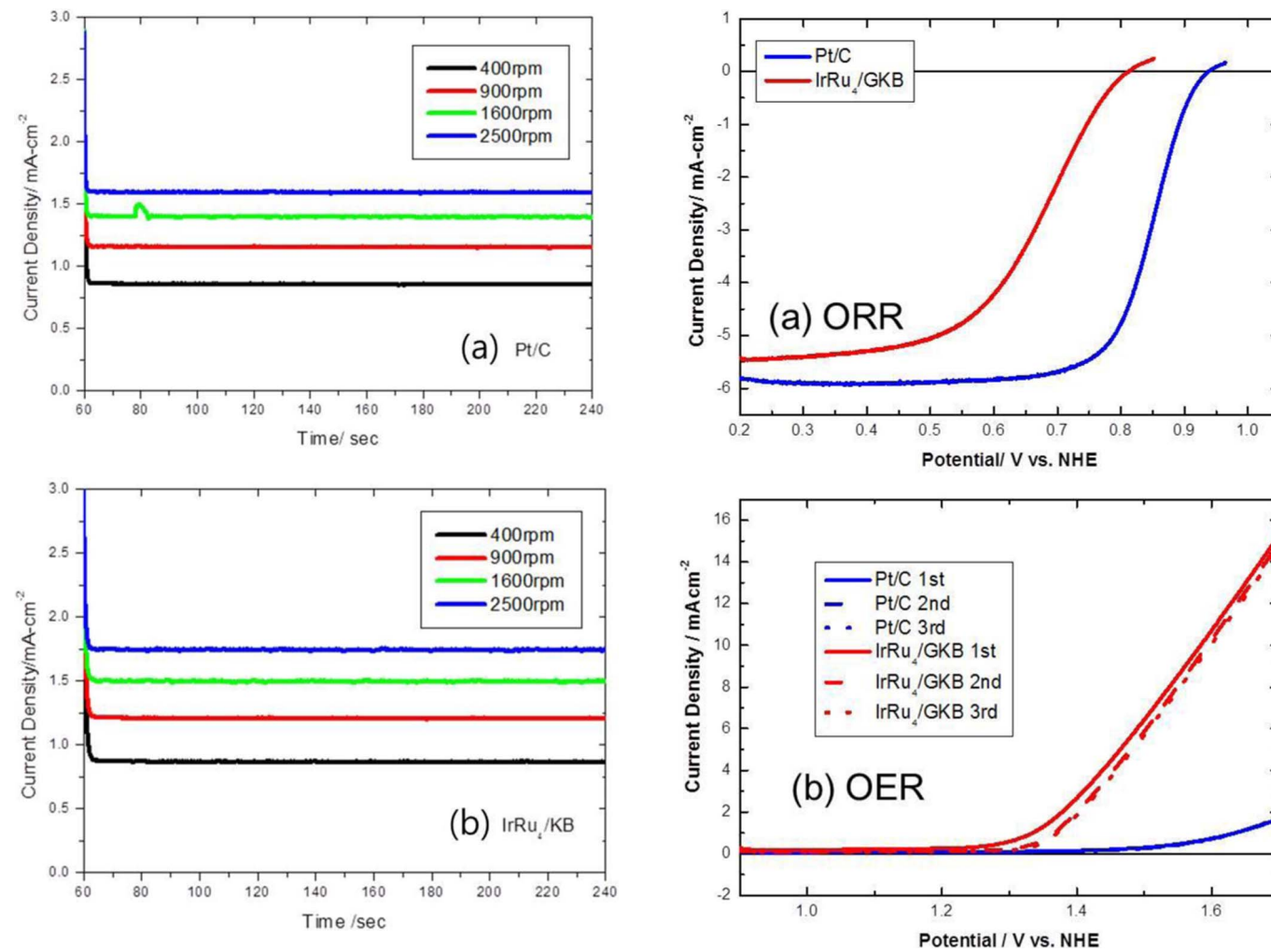


Figure 3. TEM image of IrRu<sub>4</sub>/GKB.



**Figure 4.** Chronoamperometry curves for HOR on (a) Pt/C and (b) IrRu<sub>4</sub>/KB recorded at a fixed potential of 20 mV (vs. NHE) in  $\rm H_2$ -saturated 0.1 M HClO<sub>4</sub> at rotation speeds of 400, 900, 1600, and 2500 rpm and 25°C.

**Figure 5.** Comparison of Pt/C and IrRu<sub>4</sub>/GKB polarization curves for (a) ORR in  $O_2$ -saturated 0.1 M HClO<sub>4</sub>, (b) OER in  $N_2$ -saturated 0.1 M HClO<sub>4</sub> at 1600 rpm and 25°C. Scan rate: 5 mV/s.

catalysts (Ir:Ru = 1:0, 1:1, 1:4, 1:6, 1:9, 0:1 (mol/mol)), that with Ir:Ru = 1:4 showed the best HOR activity, which was superior to that of PtRu/C. Herein, we compared the HOR activities of Pt/C and assynthesized IrRu<sub>4</sub>/KB using the RDE half-cell set-up (Fig. 4), with the obtained  $i_k$  values of IrRu<sub>4</sub>/KB and Pt/C (5.07 and 3.85 mA/cm², respectively) showing that the former catalyst showed a  $\sim$ 132% higher HOR activity than the latter one, as previously reported by Jin et al. <sup>21</sup> Thus, IrRu<sub>4</sub> was proven to be an excellent candidate to substitute Pt in MEA anodes.

*ORR activity testing.*—Although IrRu<sub>4</sub>/GKB was primarily intended for use as an HOR catalyst, its ORR activity was also measured. Fig. 5a shows the LSV curves for IrRu<sub>4</sub>/GKB and Pt/C, which exhibited ORR onset potentials of 0.812 and 0.938 V (vs. NHE) and half-maximum limiting current potentials of 0.675 and 0.848 V (vs. NHE), respectively. Based on the obtained results, it was inferred that IrRu<sub>4</sub> exhibited a certain ORR activity, although not being as active as Pt. Nonetheless, under SU/SD conditions, the IrRu<sub>4</sub>/C anode may still offer better cathode catalyst durability than the Pt/C anode.

*OER activity testing.*—Min et al.<sup>15</sup> have performed a study of OER catalysts, scrutinizing a wide spectrum of Ir and Ru bimetals and their oxides and describing their syntheses and OER activities to show that Ir<sub>1</sub>Ru<sub>1</sub>O<sub>x</sub>/C exhibited an optimal combination of OER activity and stability. Moreover, the above work demonstrated that

 $IrRu_4/C$  showed the best initial OER performance among Ir and Ru bimetals, confirming the effectiveness of this alloy as an effective OER catalyst.

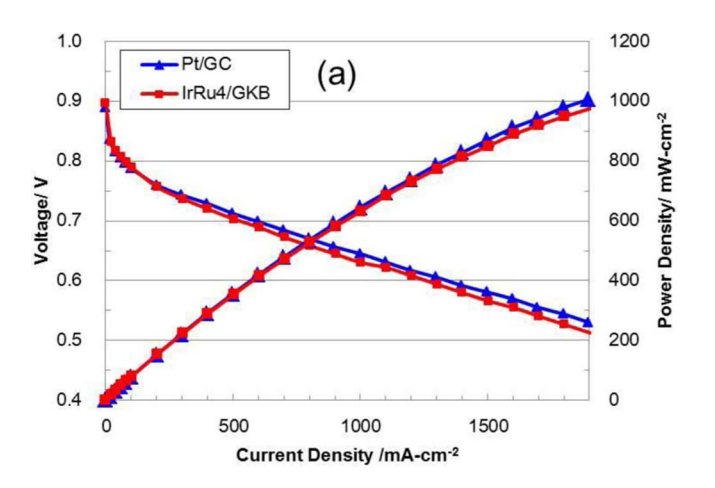
Herein, OER activity was evaluated in a half-cell set-up to compare Pt/C and as-synthesized IrRu<sub>4</sub>/GKB catalysts, with the corresponding LSV curves (Fig. 5b) showing that the OER onset potential of IrRu<sub>4</sub>/C (1.3–1.4 V vs. NHE) was much lower than that of Pt/C (1.6 V vs. NHE). Moreover, IrRu<sub>4</sub>/C achieved a current density one order of magnitude higher than that of Pt/C, which further verified that the former outperformed the latter as a water oxidation catalyst. As far as stability is concerned, the OER activity of IrRu<sub>4</sub>/C was degraded by three consecutive LSV scans, although the degradation seemed to slow down after the second scan. The activity loss was ascribed to the dissolution of Ru at high potentials. 15 Notably, Atanasoski et al. compared the OER properties of Ir and Ru,<sup>22</sup> and demonstrated that Ru outperformed Ir in terms of activity, whereas an opposite trend was observed for stability. Therefore, the above researchers concluded that the addition of a small amount of Ru should further improve the OER activity of Ir, while the addition of a suitable amount of Ir should protect Ru from extremely fast dissolution. Herein, OER testing was performed using an LSV swing of up to 1.5 V vs. Ag/AgCl, which is a very high potential ( $\sim$ 1.697 V vs. NHE). Thus, we ascribed the noticeable activity loss in the second scan to the dissolution of Ru at this high potential. A further activity loss could also be observed

Table I. Cost, performance, and anode durabilities of Pt- and IrRu <sub>4</sub> -ano
--

	PGM loading	Anode resistance mOhm cm <sup>2</sup>		MEA Power Density W/cm <sup>2</sup> @ 0.65 V	Anode tolerance
Anode catalyst	mg/cm <sup>2</sup>	65°C, 100% RH	90°C, 50% RH, 150 kPa	90°C, 50% RH, 150 kPa	$t_{\rm CR}$
Pt/GC	0.02	50	76	1.1	~1.5 min
IrRu4/GKB	0.06	80	73	1.1	$\sim$ 3 h
IrRu4 vs. Pt	65% cost	63% activity	>100% activity	100% performance	$>$ 120 $\times$ durability

in subsequent scans, although it was not as abrupt as that in the second scan. This activity loss can be explained by the dissolution of unstable Ru in the outermost layer during the first LSV scan and by the protection of the internal Ru from extreme dissolution by stable lr. Nevertheless, at high potentials, both Ru and Ir dissolution may still occur at a slower rate, regardless of IrRu<sub>4</sub>/C functioning as an OER catalyst. In addition, since the PtRu nanoparticles in the supported catalyst applied to the DMFC and residential PEMFC were of a random alloy type, exposure of the catalyst to methanol at a high voltage resulted in Ru dissolution, the extent of which was previously reported to be proportional to the extent of MEA performance degradation. 23,24 However, the IrRu<sub>4</sub> nanoparticles used herein seemed to have a coreshell structure with an Ir-rich shell, as suggested by previous extended X-Ray absorption fine structure analysis. 21 Thus, it was anticipated that the dissolution of Ru from the IrRu<sub>4</sub>-supported catalyst should not be very significant.

*I-V performance comparison.*—Single-cell *I-V* and anode polarization curves are shown in Figs. 6 and 7, respectively, and the



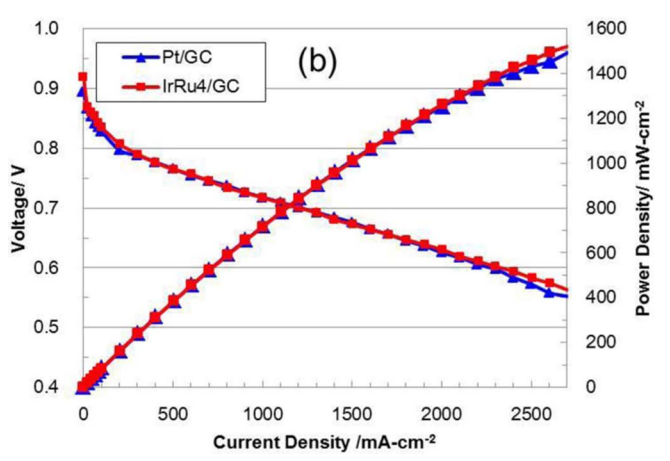


**Figure 6.** *I-V* performances of Pt/C and IrRu<sub>4</sub>/GKB anode MEAs at (a)  $65^{\circ}$ C, 100% RH, 0 kPa, anode/cathode =  $H_2/air$  = SR 1.5/2.0, (b)  $90^{\circ}$ C, 50% RH, 150 kPa, anode/cathode =  $H_2/air$  = SR 1.2/2.0.

corresponding results are summarized in Table I. Note that the internal resistance was not corrected. Both Pt and IrRu<sub>4</sub> anode–based MEAs performed better at 90°C, 50% RH, and 150 kPa than at 65°C, 100% RH, and 0 kPa. The respective open-circuit voltages (OCVs) for Pt/IrRu<sub>4</sub> MEAs (0.890/0.896 and 0.894/0.918 V) indicated that the two MEAs exhibited a negligible OCV difference. Thus, the performances of these two anode catalysts were almost identical at 90°C, 50% RH, 150 kPa, whereas Pt/C outperformed IrRu<sub>4</sub>/C at 65°C, 100% RH, and 0 kPa.

Anode polarization curves (Fig. 7) showed a linear I-V relationship within the observed range, with the slope of the I-V curve corresponding to anodic resistance. Since the same cathode catalyst layer and the membranes were used for two different anode MEAs, it was assumed that the observed difference reflected the different anode activities of the two MEAs. Although the anodic resistance was larger for IrRu<sub>4</sub>/C than for Pt/C at 65°C and 100% RH, similar values were observed at 90°C, 50% RH, and 150 kPa. Pt/C exhibited higher anodic resistance at 90°C, 50% RH, and 150 kPa than at 65°C, 100% RH, and 0 kPa, with the opposite trend observed for IrRu<sub>4</sub>/C. The above distinction may be related to the individual or combined effects of temperature, humidity, or pressure within the MEA, since operating conditions affect the activity of the catalyst for electrochemical H<sub>2</sub> adsorption, H<sub>2</sub> molecule dissociation, and adsorbed hydrogen atom charge transfer. From a macroscopic point of view, operating conditions significantly affect the activity of the cathode catalyst layer, which, in turn, affects that of the anode catalyst layer due to the existence of a water balance between the two electrodes. Currently, we are investigating the use of electrochemical impedance spectroscopy to determine the effect of operating conditions on the HOR mechanism of each catalyst.

CR (fuel starvation) test.—After basic I-V performance measurements, each MEA was tested for CR durability. Figure 8 and Table I show the CR tolerance test results of Pt- and IrRu<sub>4</sub>-anode MEAs. Two different carbon supports were used for each metal: a regular one (for Pt/C and IrRu<sub>4</sub>/KB) and that comprising graphitized carbon (for Pt/GC and IrRu<sub>4</sub>/GKB). In general, IrRu<sub>4</sub>/C exhibited a much

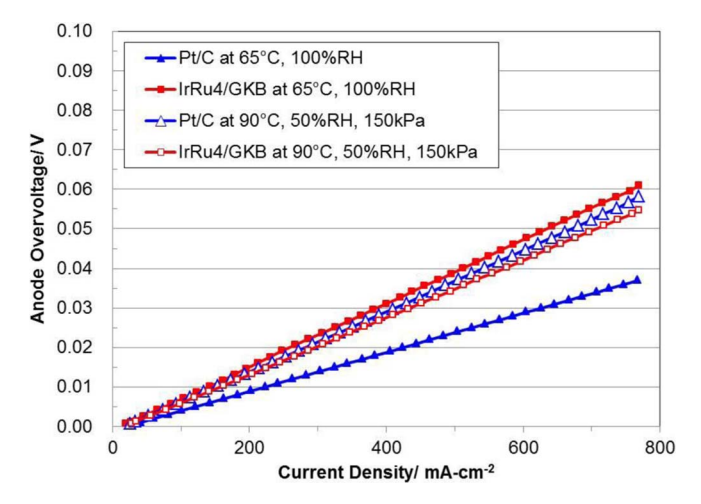


**Figure 7.** Anode polarization curves of Pt/C and  $IrRu_4/GKB$  anode MEAs at 65°C, 100% RH, 0 kPa (filled symbols) and 90°C, 50% RH, 150 kPa (empty symbols).

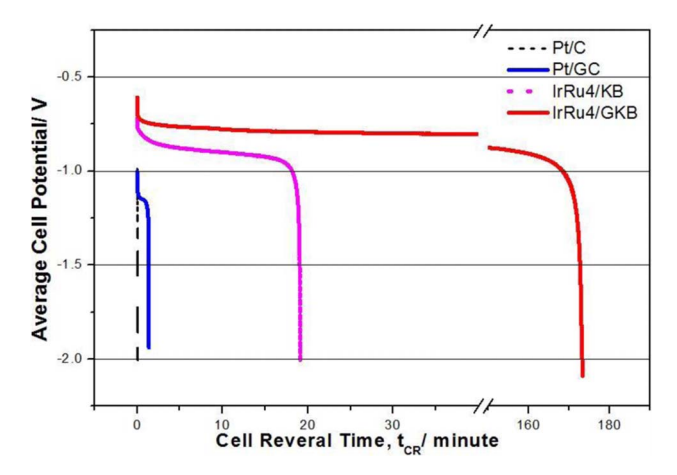


Figure 8. Durabilities of Pt/C, Pt/GC, IrRu<sub>4</sub>/KB, and IrRu<sub>4</sub>/GKB anodes under CR conditions.

higher anode durability than Pt/C regardless of the support type. In particular, IrRu<sub>4</sub>/GKB lasted ~3 h before the cell potential reached -2.0 V, whereas Pt/GC lasted only several minutes. Thus, the use of a graphitized carbon support was not effective in increasing the durability of Pt under the harsh conditions of fuel starvation. In a separate experiment, when the Pt loading was increased from 0.02 to 0.05  $mg_{Pt}/cm^2$ ,  $t_{CR}$  increased only by several minutes. This incomparable durability difference between the two catalysts was ascribed to the ability of IrRu<sub>4</sub>/C to promote water oxidation over carbon corrosion. The plateau in the potential range from -0.75 to -0.9 V depicted in Fig. 8 for IrRu<sub>4</sub>/C indicates that water oxidation (i.e., OER) took place to sustain the current. For Pt/C, the plateau was observed at a slightly more negative potential (-1.1 V) due to the lower OER activity of Pt. It was speculated that two competing reactions, OER and COR (Equations 1 and 2) occurred within the plateau region, being possibly accompanied by metal oxidation. IrRu<sub>4</sub>/GKB was believed to last longer than IrRu<sub>4</sub>/KB due to being supported by graphitized carbon, which is more stable toward oxidation than Ketjen black. This result confirmed that  $t_{CR}$  is significantly influenced by both catalyst material and supporting material durability. The incorporation of an OER catalyst such as IrO2 into the Pt/C-based anode drastically enhanced the CR durability of MEAs, with the above increase being positively correlated with OER catalyst loading.<sup>16</sup> Since IrRu<sub>4</sub> exhibits a certain OER activity in the absence of other components, the IrRu<sub>4</sub>-anode MEA should feature a better self-protection capability than the Pt-anode one under unexpected CR conditions.

Even though CO tolerance of anode catalysts was not investigated herein, it is of high importance for PEMFCs or direct alcohol fuel cells, because some applications utilize reformed fuel gas mixtures containing CO as an impurity instead of pure H<sub>2</sub> as PEMFC stack fuel. Moreover, CO is a by-product of alcohol oxidation in direct alcohol fuel cells, and it can poison the active sites of the Pt catalyst and thereby lower the fuel cell performance. CO oxidation is known to be favored by oxophilic materials such as Ru because of the presence of -OH groups on their surface that promote the electrochemical conversion of CO to CO<sub>2</sub>. <sup>17,25</sup> In view of the above, PtRu/C is considered to be a state-of-the-art PEMFC anode catalyst for stationary applications, and is used in preference to Pt/C in PEMFCs or direct alcohol fuel cells. Although this is not the case for FCEVs, which are fueled with pure H<sub>2</sub> most of the time, in cases when reformate gas is used, the IrRu<sub>4</sub>/C anode should potentially show a higher CO tolerance than the Pt/C anode because it is heavily loaded with Ru.

#### Conclusions

Herein, we described the preparation and physico-electrochemical properties of an IrRu<sub>4</sub>/C anode catalyst and evaluated its applicability to single-cell PEMFCs. When IrRu<sub>4</sub>, featuring a relatively low base material cost (66% that of Pt), was used as the anode electrocatalyst, a Pt-comparable MEA performance was observed. Moreover, IrRu<sub>4</sub>/C acted not only as an HOR-enabling anode catalyst during normal fuel cell operation, but also functioned as an OER-active catalyst when cell reversal tolerance was in demand. Thus, this work showed that IrRu<sub>4</sub>/C is an outstanding candidate for replacing Pt/C in anodes of automotive PEMFCs in terms of cost, performance, and durability.

#### Acknowledgments

We express our sincere gratitude to our colleagues from the Materials R&D Analysis Group, particularly to Dr. Kwangjong Suh for coordinating the analysis and helpful advice, Min-Jin Song for performing ICP analyses, and Jong-Min Kim for TEM imaging. Support from the Samsung SDI Battery R&D Center is gratefully acknowledged. C. Pak also thanks GIST Research Institute (GRI) grant funded by the GIST in 2018.

#### ORCID

Chanho Pak https://orcid.org/0000-0002-4075-0477

#### References

- 1. A. Serov and C. Kwak, Appl. Catal. B, 90, 313 (2009).
- D. Yang, B. Li, H. Zhang, J. Zheng, R. Lin, and J. Ma, J. Power Sources, 199, 68 (2012).
- 3. K. Kwon, S.-A. Jin, K. H. Lee, D. J. You, and C. Pak, *Catal. Today*, **232**, 175 (2014).
- P. P. Patel, M. K. Datta, O. I. Velikokhatnyi, P. Jampani, D. Hong, J. A. Poston, A. Manivannan, and P. N. Kumta, J. Mater. Chem. A, 3, 14015 (2015).
- J. Durst, A. Orfanidi, P. J. Rheinländer, F. Hasché, C. Eickes, P. Suchsland, M. Binder, and H. A. Gasteiger, ECS Trans., 69, 67 (2015).
- R. T. Atanasoski, G. D. Vernstrom, G. M. Haugen, T. M. Watschke, J. M. Wheldon, S. M. Hendricks, L. L. Atanasoska, and A. E. Hesteret, FY 2011 Annual Progress Report of DOE Hydrogen and Fuel Cells Program, V.D.3 (2011).
- 7. C. Qin, J. Wang, D. Yang, B. Li, and C. Zhang, Catalysts, 6, 197 (2016).
- Y. Yu, H. Li, H. Wang, X.-Z. Yuan, G. Wang, and M. Pan, J. Power Sources, 205, 10 (2012).
- P. T. Yu, W. Gu, R. Makharia, F. T. Wagner, and H. A. Gasteiger, ECS Trans. 3, 797 (2006).
- 10. H. Chhina, S. Campbell, and O. Kesler, J. Power Sources, 179, 50 (2008).
- 11. H. Chhina, S. Campbell, and O. Kesler, J. Power Sources, 161, 893 (2006).
- K. Eom, Y. Y. Jo, E. Cho, T.-H. Lim, J. H. Jang, H.-J. Kim, B. K. Hong, and J. H. Lee, J. Power Sources, 198, 42 (2012).
- 13. J.-G. Oh, W. H. Lee, and H. Kim, Int. J. Hydrogen Energy, 37, 2455 (2012).
- R. T. Atanasoski, D. A. Cullen, G. D. Vernstrom, G. M. Haugen, and L. L. Atanasoska, ECS Electrochem. Lett., 2, F25 (2013).
- M. Min, N.-W. Kong, E. You, T.-Y. Kim, and C. Pak, ECS Meeting Abstracts, MA2014-02 1072 (2014).
- B. K. Hong, P. Mandal, J.-G. Oh, and S. Litster, J. Power Sources, 328, 280 (2016).
- K. H. Lim, W. H. Lee, Y. Jeong, and H. Kim, J. Electrochem. Soc., 164, F1580 (2017).
- 18. T. R. Ralph, S. Hudson, and D. P. Wilkinson, *ECS Trans.* 1, 67 (2006).
- Cost calculations based on the past five years' base material price (Pt, Ir, Ru) obtained from http://www.platinum.matthey.com/ (2012–2017).
- A. J. Bard and L. R. Faulkner, Electrochemical Methods: Fundamentals and Applications, 2nd ed., p. 341, John Wiley & Sons, Hoboken, NJ (2001).
- 21. S. A. Jin, C. Pak, D. J. Yoo, and K. H. Lee, US 2013/0137009 A1, (2013).
- R. T. Atanasoski, L. L. Atanasoska, D. A. Cullen, G. M. Haugen, K. L. More, and G. D. Vernstrom, *Electrocatal.*, 3, 284 (2012).
- G.-S Park, C. Pak, Y.-S. Chung, J.-R. Kim, W. S. Jung, Y.-H. Lee, K. Kim, H. Chang, and D. Seung, *J. Power Sources*, 176, 484 (2008).
- Y. Chung, C. Pak, G.-S. Park, W. S. Jeon, J.-R. Kim, Y. Lee, H. Chang, and D. Seung, J. Phys. Chem. C, 112, 313 (2008).
- 25. H. A. Gasteiger, N. Markovic, and P. N. Ross Jr., J. Phys. Chem., 99, 8290 (1995).